SOILS AND FOUNDATIONS Vol.26, No.1, 65-84, Mar. 1986
Japanese Society of Soil Mechanics and Foundation Engineering

STRENGTH AND DEFORMATION CHARACTERISTICS OF SAND IN PLANE STRAIN COMPRESSION AT EXTREMELY LOW PRESSURES

Fumio Tatsuoka*, Makoto Sakamoto**, Taizo Kawamura***
and Shinji Fukushima****

ABSTRACT

A series of drained plane strain compression tests was performed on saturated samples of fine angular to sub-angular sand at confining pressures from 0.05 kgf/cm^2 (4.9 kN/m^2) up to 4.0 kgf/cm^2 (392 kN/m^2). Samples were prepared by the air-pluviation method with changing the angle δ of bedding plane to the σ_1'-direction during plane strain compression tests from 0 to 90 degrees. It was found that in the plane strain compression tests the dependency of $\phi=\arcsin\{(\sigma_1'-\sigma_3')/(\sigma_1'+\sigma_3')\}_{max}$ on σ_3' is very small when σ_3' is lower than around 0.5 kgf/cm^2 as well as in the triaxial compression tests. Strong strength anisotropy was observed; ϕ has its minimum at δ between 23° and 34°. It was also found that this minimum value of ϕ in plane strain compression is similar to ϕ at this value of δ in triaxial compression. The tendency of such strength anisotropy was found rather insensitive to stress levels employed ($\sigma_3'=0.05\sim4.0$ kgf/cm^2). The stress-dilatancy relation at the peak stress condition was found to be a strong function of δ whereas this relation was insensitive to the change of σ_3'. The change of the deformation characteristics of sample with the change of σ_3' was found to be rather small when σ_3' is lower than around 0.5 kgf/cm^2 as well. It was found that the strength anisotropy and deformation anisotropy as a function of δ are somewhat different.

Key words : angle of internal friction, dilatancy, drained shear, plane strain compression test, sand, shear strength (**IGC** : D 6)

INTRODUCTION

To analyze the results of small model tests under the plane strain condition in normal gravity, the anisotropic strength and deformation characteristics of the model sand at

* Associate Professor, Institute of Industrial Science, University of Tokyo, 22-1, Roppongi 7, Minato-ku, Tokyo 106.
** Engineer, Ministry of Construction. Formerly Graduate Student of University of Tokyo.
*** Research Engineer, Hitachi Zosen Corp. Formerly Visiting Research Personnel of University of Tokyo.
**** Research Engineer, Fujita Technical Labo., Fujita Corp. Formerly Graduate Student of University of Tokyo.
Manuscript was received for review on July 5, 1985.
Written discussions on this paper should be submitted before October 1, 1986, to the Japanese Society of Soil Mechanics and Foundation Engineering, Sugayama Bldg. 4 F, Kanda Awaji-cho 2-23, Chiyoda-ku, Tokyo 101, Japan. Upon request the closing date may be extended one month.

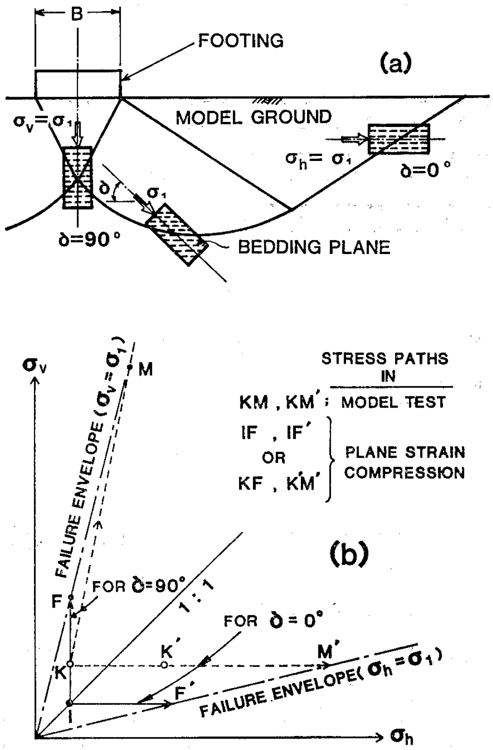

Fig. 1. Schematic diagram showing (a) the σ_1'-direction at failure and (b) stress paths for $\delta=0°$ and 90° in a model bearing capacity test

extremely low pressures are needed (Fig. 1). To this end, two series of triaxial compression tests have been performed by the authors and their colleagues. First, the dependency of the strength and deformation characteristics of the model sand (Toyoura Sand) on the minor principal stress σ_3' was investigated by Fukushima and Tatsuoka (1984). It was found that the value of $\varphi=\arcsin\{(\sigma_1'-\sigma_3')/(\sigma_1'+\sigma_3')\}_{max}$ and the deformation characteristics are rather independent of σ_3' for a stress range of $\sigma_3'\fallingdotseq 0.05\sim 0.5$ kgf/cm² (5~50 kN/m²). Then, Tatsuoka et al. (1986) investigated the effects of several factors on the strength and deformation characteristics of the model sand by triaxial compression tests at low stress levels ($\sigma_3'=0.05\sim 1.0$ kgf/cm²). These tests were needed because while at the authors' laboratory in model tests the same mass of air-dry Toyoura Sand had been used repeatedly, the plane strain compression tests were performed on fresh saturated samples which were prepared by the freezing method which will be described in the later part. It was found that even at these low stress levels, the effects of these factors (frozen or unfrozen during sample preparation, air-dry or saturated during test, and fresh or used sand) on the results are very small.

On the other hand, Arthur and Assadi (1977) and Oda et al. (1978 and 1981) showed that the degree of strength anisotropy is larger in plane strain compression than in triaxial compression. In the tests by Oda et al. (1978), the minimum values of φ were recorded for $\delta=24°\sim 30°$ (δ=the angle of bedding plane to the σ_1'-direction, Fig. 1) at $\sigma_3'=2.0$ and 4.0 kgf/cm². The existence of such a minimum was also shown by Matsuoka et al. (1984). However, the minimum of φ at $\delta=24°\sim 30°$ is not clear in the data at $\sigma_3'=0.5$ and 1.0 kgf/cm² by Oda et al. (1978), in those at $\sigma_3'=0.5$ and 3.0 kgf/cm² by Kimura et al. (1985) and in those at $\sigma_3'\fallingdotseq 0.5$ kgf/cm² by Arthur and Assadi (1977). Therefore, to clarify how such strength anisotropy as above depends on the stress level, a more comprehensive series of tests was considered necessary.

Furthermore, it has not been well under stood how φ of the model sand depends on σ_3' at low stress levels in plane strain compression. This kind of information is needed for a wide range of σ_3', say $0.05\sim 1.0$ kgf/cm² (5~100 kN/m²), for the analysis of the results of small model tests in normal gravity. So far, only a very limited number of the test results has been reported in literature (for example, van Leussen and Nieuwenhuis, 1984).

In view of the above, a series of drained plane strain compression tests was performed on air-pluviated saturated fresh Toyoura Sand for a wide range of σ_3' from 0.05 to 4.0 kgf/cm² (4.9 to 392 kN/m²) with changing δ (0°~90°) at each value of σ_3'.

TEST PROCEDURES

Two series of tests were performed. The first series (Series A) was performed by

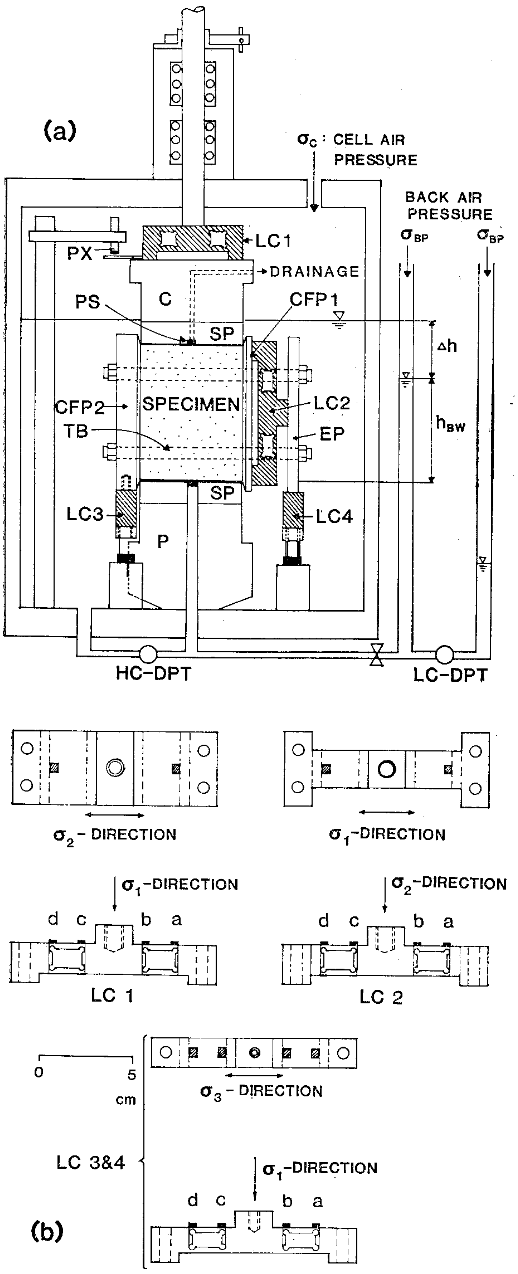

Fig. 2. Schematic diagrams of (a) plane strain compression apparatus and (b) load cells used in tests at $\sigma_3'=0.05$ and $0.1\,kgf/cm^2$ (HC-DPT ; high-capacity differential pressure transducer to measure σ_c' and LC-DPT ; low capacity differential pressure transducer to measure volume change) ($1\,kgf/cm^2=98\,kN/m^2$)

second and third authors and the second series (Series B) was performed by the last author.

Series A

The nominal initial sample dimensions are h_0 (height) $=10.5$ cm, w_0 (width or length in the σ_3'-direction) $=4$ cm and l_0 (length in the σ_2'-direction) $=8$ cm (Sample A). A ratio $h_0/w_0=2.6$ was employed to minimize the effects of end friction on the results, especially measured strength values. The stainless steel plate (SP, see Fig. 2(a)) having a drainage hole with a diameter of 5 mm for a porous stone (PS) was glued to the cap and pedestal of duralumin and its rectangular surface was sufficiently polished to better the lubrication quality. The confining plates (CFP 1 and CFP 2) were made of stainless steel and their surfaces were also sufficiently polished. Based on the study of Tatsuoka, Molenkamp, Torii and Hino (1984), the composition of lubrication layer was changed depending on the maximum normal stress in the plane strain compression test. Type 1 with Silicone grease KS 63 G was employed for the tests at $\sigma_c'=0.05$ and $0.1\,kgf/cm^2$ and Type 1 with Dow grease was used for the tests at $\sigma_c'=0.5$, 1.0 and $4.0\,kgf/cm^2$.

While the major parts of the test procedures in this study were the same as the previous studies (Fukushima and Tatsuoka, 1984 ; Tatsuoka, Goto and Sakamoto, 1986), the following modifications were made.

(1) For the tests at $\sigma_c'=0.05$ and $0.1\,kgf/cm^2$, four load cells (LC 1, LC 2, LC 3 and LC 4 shown in Figs. 2(a) and 2(b)) were newly built based on the original idea of Tani et al. (1983) to measure the boundary loads of sample inside the triaxial cell. All these load cells were machined from lumps of phosphor bronze. The load cell LC 1 is to measure the axial load of sample, which is very similar to the one used in the triaxial compression tests at $\sigma_c'=0.05\,kgf/cm^2$ by Tatsuoka et al. (1986). The load cell LC 2 is to measure the horizontal load $Q=(\sigma_2'-\sigma_3')\times(w\times h$; the side area of sample). Since the load cell LC 2 supports directly the confining plate CFP 1, all the load Q is directly transmitted to LC 2. The plates CFP 2 and EP (Fig. 2(a)) are connected by four tie-

bars (TB). The seating stress of the confining plates at their setting was also controlled by means of LC 2. The load cell LC 2 was used in thirteen tests at $\sigma_c'=0.05$ kgf/cm^2. In the other tests at $\sigma_c'=0.05$ kgf/cm^2 and tests at $\sigma_c'=0.1$ kgf/cm^2, CFP 1, LC 2 and EP were replaced with an acryl plate to measure the strain field of sample on the σ_2'-plane, since either the measurement of σ_2' or the measurement of strain field was possible in the configuration of the apparatus employed in this study. The load cells LC 3 and LC 4 measure the total vertical friction working on the confining plates (CFP 1 and CFP 2). The head and two legs of each load cell were tightly connected to other rigid parts. In each load cell, four active strain gages labelled *a*, *b*, *c* and *d* form a Wheatstone bridge. This configuration has been found to be very effective to make the load cell very sensitive to the normal load to be measured but very insensitive to other load components (Tatsuoka et al., 1986). It was carefully confirmed that each load cell has a high linearity and a high rigidity. For example, the rigidities of LC 1 and LC 2 were found to be 0.42 kgf/μm and 0.22 kgf/μm, which are rather large values since the capacity is very small (20 kgf). By means of these four load cells or three load cells (LC 1, LC 3 and LC 4) together with a proximeter (PX), the stress path and axial deformation during the sample preparation phase and the isotropic compression phase were carefully monitored and controlled.

For the tests at σ_c' equal to and larger than 0.5 kgf/cm^2, a conventional load cell placed outside the triaxial cell was used to measure the axial loads and the load cells LC 2, LC 3 and LC 4 were not used. The weights of the confining plates were supported by coil springs in place of LC 3 and LC 4 so that the plates are in a floating condition. With this arrangement, vertical friction τ_v on the confining plates works in the same direction only along a half height of sample, resulting in reduced effects of the vertical friction on the measured stress values. When $\tau_v=0.004$ kgf/cm^2 is assumed based on the results by Tatsuoka et al. (1984), the effects of τ_v on the measured value of φ becomes negligible for $\sigma_c'\geqq 0.5$ kgf/cm^2. In all the tests at $\sigma_c'\geqq 0.5$ kgf/cm^2, an acryl plate was used as a confining plate (CFP 1) to measure the strain field of sample on the σ_2'-plane.

(2) In the tests at $\sigma_3'=0.05$ and 0.1 kgf/cm^2, the cell air pressure σ_c and the back air pressure σ_{BP} with both being 0.5 kgf/cm^2 were supplied from the same source so that both values are exactly the same (Tatsuoka et al., 1986). The positive effective confining pressure $\sigma_c'=\sigma_c-\sigma_{BP}+\gamma_w\cdot\Delta h$ (Fig. 2(a)) was produced by locating the water level in the burette lower than the cell water level. Therefore, the value of σ_3' was calculated as

$$\sigma_3'=\sigma_c'+\Delta\sigma_3 \tag{1}$$

where σ_c' is the pressure difference between the cell water pressure and the pore water pressure as measured with a HC-DPT (Fig. 2(a)) and $\Delta\sigma_3$ is the stress correction described later. The value of σ_c' was kept constant during a plane strain compression test by adjusting the level of the burette continuously.

Except for two tests at $\sigma_c'=0.5$ kgf/cm^2, all the samples were nearly isotropically consolidated at $\sigma_c'=0.05$, 0.1, 0.5, 1.0 and 4.0 kgf/cm^2 before plane strain compression. Of course the stress condition within a sample cannot be perfectly isotropic due to the self-weight, the membrane forces and the seating stress of the confining plates. On the other hand, the stress paths in these plane strain compression tests which are denoted by IF or IF' in Fig. 1(b) are different from those in model tests which are denoted, for example, by KM and KM' for $\delta=90°$ and 0°. Since the stress paths at various points in the model ground are difficult to be exactly simulated in element tests, an identical simplest stress path was employed in this study for all values of δ(0°$\sim$90°) where σ_1' is increased with a constant σ_3' starting from the nearly isotropic condition ; $\sigma_1'\fallingdotseq\sigma_2'\fallingdotseq\sigma_3'$.

To confirm whether the initial stress condition, isotropic or anisotropic, has effects on the plane strain compression strength, two tests were performed where samples of $\delta=90°$ were first anisotropically consolidated at a stress condition, $\sigma_{1c}'=0.5/K_0$ kgf/cm^2 and $\sigma_{2c}'=\sigma_{3c}'=0.5$ kgf/cm^2 where σ_{1c}', σ_{2c}' and σ_{3c}' are the major, intermediate and minor principal stresses during consolidation. The value of K_0 was determined based on an empirical relation $K_0=0.52\,e$ obtained by O-kochi and Tatsuoka (1984).

Series B

Two types of samples were used:

(a) (Sample BS) samples having dimensions of $h_0 \times l_0 \times w_0=8.0\times8.0\times4.3$ (cm) with the ends being lubricated by Type 1 using Silicone grease KS 63 G, and

(b) (Sample BM) samples having dimensions of $h_0 \times l_0 \times w_0=10.1\times10.3\times5.5$ (cm) with the ends being lubricated by Type 1 or Type 2 using Dow grease.

All the samples were anisotropically consolidated with $\sigma_{3c}'/\sigma_{1c}'=K_0=0.52\,e$. For Sample BS, $\sigma_{1c}'=2.0$ and 4.0 kgf/cm^2 were employed for $\delta=90°$, while only $\sigma_{1c}'=2.0$ kgf/cm^2 was employed for $\delta=0°$. The values of σ_2' were measured in the tests at $\sigma_{1c}'=2.0$ kgf/cm^2. For Sample BM, only $\sigma_{1c}'=2.0$ kgf/cm^2 was employed without measuring σ_2'. The other test procedures are the same as the tests at $\sigma_c'\geqq0.5$ kgf/cm^2 in Series A.

SAMPLE PREPARATION

By the following two reasons, the freezing method was employed. First, in this study conventional latex membranes having a circular cross-section were used for simplicity. Membranes were sealed at the cylindrical portions of the cap and the pedestal. With this kind of membrane, it is rather difficult to make a good contact at their vertical corners between membrane and the inner surface of mold by vacuuming the space between them. Secondly, it is apparent that samples of δ other than 90° cannot be made by the conventional air-pluviation method.

In the freezing method, sand particles were poured through air into the inner room of mold of duralumin without a membrane. For $\delta=90°$ and 0°, the mold consisting of five plates is not tilted. For other values of δ, the following procedures were employed (Fig. 3) : (1) First, the mold with one side plate having been removed, thus consisting of four plates, is placed in an acryl box which has been tilted at a prescribed angle of δ. (2) Then, sand is poured until the mold is completely buried in sand. (3) The whole sand mass placed in the acryl box is moistened with a head at the bottom being 2～3 cm of water. (4) One surface of the sample is smoothed and flattened by scraping carefully with a thin steel blade. Since sand is moist at this moment, the disturbance by this procedure seems very small. (5) One side plate is fixed to the remaining part of the mold. (6) The acryl box together with the mold and sand is rotated gently to the vertical position. Again, the disturbance seems very small as well as at Step (4). Then, the top surface of the sample is smoothed and flattened.

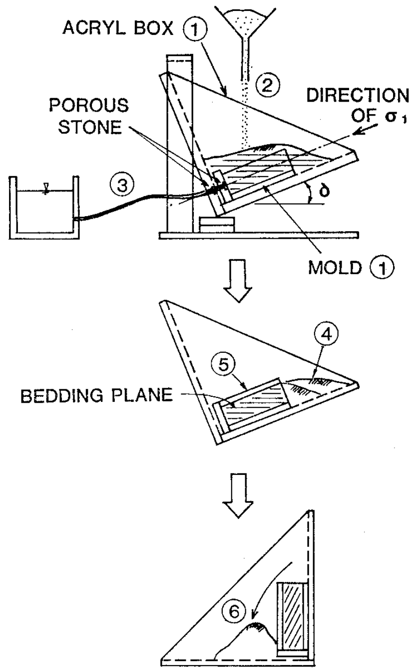

Fig. 3. Procedures to prepare samples of δ other than 0° and 90°

After these procedures, all kinds of moist samples of $\delta=0°\sim90°$ together with the mold are put into a freezer at $-20°C$. Several cares taken to avoid the expansion of the volume of sample during freezing are described in detail in Tatsuoka et al. (1986). A frozen sample sealed to the cap and the pedestal with a latex membrane of a thickness of 0.2 mm or 0.3 mm was thawed at a room temperature of 20°C at a vacuum of 0.05 kgf/cm² (4.9 kN/m²) under the isotropic stress condition. Then, the sample dimensions were measured for defining the initial void ratio $e_{0.05}$.

The confining plates were set when a sample was vacuumed either at an effective confining pressure σ_c' at which the plane strain compression test was performed when $\sigma_c' \leqq 0.5$ kgf/cm² or at $\sigma_c'=0.8$ kgf/cm² when $\sigma_c'=1.0$ or 4.0 kgf/cm². In the latter case, the σ_2'-plane of sample may depart from the confining plate(s) when σ_c' increases from 0.8 kgf/cm² to 1.0 or 4.0 kgf/cm². The horizontal normal strain during this isotropic compression for $\sigma_c'=0.8 \sim 4.0$ kgf/cm² calculated from the measured volume change and axial compression was only between 0.06 and 0.21% with an average of 0.14%. Furthermore, any departure between the sample and the confining plate(s) during the isotropic compression was not observed with naked eyes. Therefore, it was considered that even in the tests at $\sigma_c'=1.0$ and 4.0 kgf/cm², the plane strain condition was maintained except for the very beginning of shearing.

Plane strain compression tests were performed at an axial strain rate of $\dot{\varepsilon}_a=0.25\%$/min. For all the tests, fresh Toyoura Sand was used which has a mean grain size of 0.16 mm, a uniformity coefficient of 1.46, a specific gravity of 2.64 and an angular to subangular shape.

STRESS CORRECTION

While the stress correction in the triaxial compression tests is not so complicated due to the cylindrical shape of sample, it is not simple in the plane strain compression tests since the membrane forces and the confining plate friction induce a non-uniform stress condition within a rectangular prism sample. Since the exact non-uniform stress distribution within a sample is very difficult to estimate, the averaged stress values σ_1' and σ_3' were calculated by the following different methods. In these methods, the forces working in the latex disks with a thickness of 0.3 mm used for lubrication at the top and bottom ends are neglected.

Method-U : Both σ_1' and σ_3' are uncorrected for both the membrane forces and the confining plate friction and are calculated as

$$\sigma_1'=(\sigma_1')_0=P/A+\gamma'\cdot z, \quad \sigma_3'=\sigma_c' \qquad (2)$$

where P is the total axial load working to the top of the sample (sand plus membrane), A is the cross-sectional area of sample$=w \times l$, z is the distance down from the top of the sample and γ' is the effective unit weight of sample. The calculated value of σ_1'/σ_3' at the bottom of sample ($z=h$) is the largest value among those calculated by these different stress calculation methods for one set of measured boundary loads and stresses.

Method C-1 : It is assumed that for the major part of sample the effective minor principal stress σ_3' is free from the horizontal forces working in the part of membrane in contact with the confining plates considering a high flexibility of the membrane. It is further assumed that the membrane has buckled for the axial load at large axial strains as in the case of some tests and the load P is supported only by the sand portion of sample. However, it is assumed that the vertical friction τ_v on the confining plate is uniformly distributed and is resisted uniformly by the whole of the sample. The values of σ_1' and σ_3' are given as

$$\sigma_1'=(\sigma_1')_0-f\cdot z, \quad \sigma_3'=\sigma_c' \qquad (3)$$

where $f=\tau_v \times h \times w \times 2/(h \times l \times w)=F/V_s=$(the total vertical load as measured by Load Cells LC 3 and LC 4)/(the volume of sample). It seems that these assumptions are more realistic at higher levels (smaller z) of sample. For tests at $\sigma_c' \geqq 0.5$ kgf/cm², the term $f\cdot z$ can be neglected.

Method C-2 : It is assumed that the shape of the membrane is of right rectangular prism during tests. In this study, membranes were set in such that initial axial strains do not exist in them. In this case, the total axial load in the membrane M can be obtained by the theory of elasticity as

$$M=2\cdot w\cdot t_m\{2\cdot E_m(2\varepsilon_1+\varepsilon_3+\varepsilon_0)/3+(\sigma_2'-\sigma_c')\}+2\cdot l\cdot t_m\cdot\{2\cdot E_m(2\varepsilon_1+\varepsilon_2+\varepsilon_0)/3\} \quad (4)$$

where E_m and t_m are the Young's modulus ($=15\,\mathrm{kgf/cm^2}$) and the thickness of membrane (0.2 mm or 0.3 mm) respectively, ε_1, ε_2 and ε_3 are the major, intermediate and minor principal strains of sample with $\varepsilon_2=0$ in the plane strain compression tests and ε_0 is the initial horizontal strain in the membrane ($\varepsilon_0<0$). This equation was derived using ν (Poisson's ratio) of membrane=0.5. The other parts of stress correction method are the same as Method C-1. The equations for σ_1' and σ_3' are

$$\sigma_1'=(\sigma_1)_0'-M/A-f\cdot z,\quad \sigma_3'=\sigma_c' \quad (5)$$

These assumptions seem also more realistic at higher levels of sample. Again the term $f\cdot z$ can be neglected in the tests at $\sigma_c'\geqq 0.5\,\mathrm{kgf/cm^2}$.

Method C-3 : It is assumed that the total axial load carried by the sand portion is $P-(M+F)$ with the other parts of stress correction method being the same as Method C-2. The equations for σ_1' and σ_3' are

$$\sigma_1'=(\sigma_1)_0'-(M+F)/A,\quad \sigma_3'=\sigma_c' \quad (6)$$

This stress correction method for the vertical friction on the confining plates F is the same as the one used by Becker, Chan and Seed (1972). This assumption may be more realistic at lower levels of sample. The term F/A can be neglected in the tests at $\sigma_c'\geqq 0.5\,\mathrm{kgf/cm^2}$.

Method C-4 : Is is assumed that the horizontal forces working in the membrane in contact with the confining plates increase σ_3' uniformly along the length of sample by the amount of $\Delta\sigma_3'$. The value of $\Delta\sigma_3'$ is obtained by the theory of elasticity as well as M (Eq. 4) ;

$$\Delta\sigma_3=-2\cdot t_m\cdot\{2\cdot E_m(\varepsilon_1+2\varepsilon_3+2\varepsilon_0)/3+(\sigma_2'-\sigma_c')\}/l \quad (7)$$

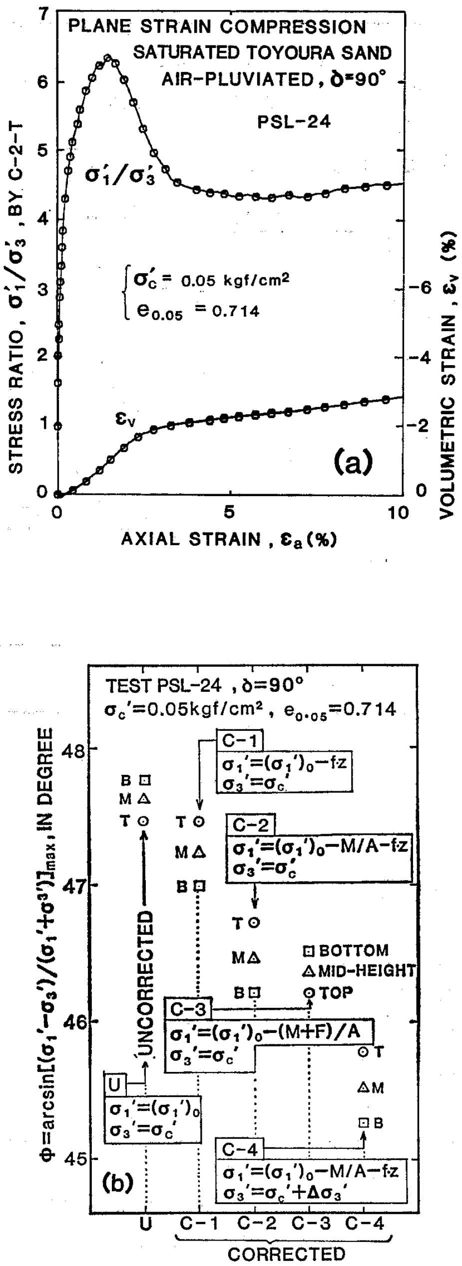

Fig. 4. (a) Typical stress-strain relations for a dense sample of $\delta=90°$ tested at $\sigma_c'=0.05\,\mathrm{kgf/cm^2}$ and (b) the values of φ calculated by different methods

In deriving Eq. (7), it is assumed that the effects of the horizontal friction on the confining plates on the deformation of membrane is negligible. The other parts of stress correction method are the same as Method C-2. The equations for σ_1' and σ_3' are

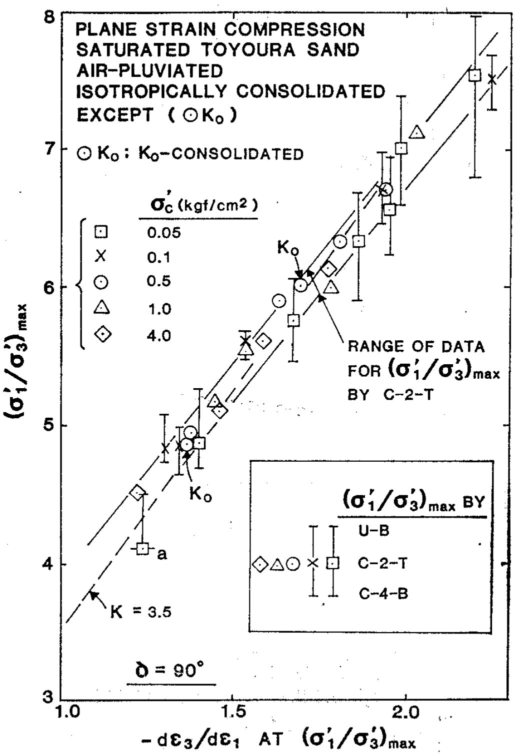

Fig. 5. Stress-dilatancy relations at $(\sigma_1'/\sigma_3')_{max}$ for $\delta=90°$ in Series A

$$\sigma_1'=(\sigma_1')_0-M/A-f\cdot z;\quad \sigma_3'=\sigma_c'+\Delta\sigma_3 \tag{8}$$

This method is essentially the same as the one employed by Duncan and Seed (1967). The term $f\cdot z$ can be neglected in the tests at $\sigma_c'\geqq 0.5$ kgf/cm^2.

The values of φ calculated by these methods for a test at $\sigma_c'=0.05$ kgf/cm^2 are compared in Fig. 4(b) where the values of φ calculated using the stress values at the top, mid-height and bottom of sample are denoted by the letters *T*, *M* and *B*. Fig. 4(a) shows the stress-strain relations for this test where the stress values were calculated by Method C-2-T (the stresses are calculated by Method C-2 at the top of sample). It may be seen in Fig. 4(b) that the largest difference in φ by the different stress calculation methods is as much as around 2.5 degrees in this case. The smallest φ or $(\sigma_1'/\sigma_3')_{max}$ is obtained by the method C-4-B (at the bottom of sample) among these different methods. Note that in the tests at $\sigma_c'\geqq 0.5$ kgf/cm^2 the difference in φ or $(\sigma_1'/\sigma_3')_{max}$ by the different methods becomes very small. At present, no clear conclusion has been obtained yet concerning which of the above methods or another is correct.

Fig. 5 shows the stress-dilatancy relations at $(\sigma_1'/\sigma_3')_{max}$ (Rowe, 1962) for the data for $\delta=90°$ obtained by the tests of Series A. It may be seen that when the values of $(\sigma_1'/\sigma_3')_{max}$ are calculated by the method C-2-T, all the data points for $\sigma_c'=0.05\sim 4.0$ kgf/cm^2 are located within a very narrow band except a data point for a very loose sample which is designated by the letter *a*. It may be seen, however, that when the values of $(\sigma_1'/\sigma_3')_{max}$ are calculated by either the methods U-B or C-4-B, such a unique relationship as for the method C-2-T cannot be obtained. For the data obtained by this study, the dependency of the stress-dilatancy relation at $(\sigma_1'/\sigma_3')_{max}$ on σ_c' was found to be the smallest for the method C-2-T. Accordingly, if we can assume that the stress-dilatancy relation at $(\sigma_1'/\sigma_3')_{max}$ is independent of σ_3' between 0.05 and 4.0 kgf/cm^2, it seems reasonable to present the data by using the stress values calculated by the method C-2-T. In the following parts, the values of σ_1', σ_3' and φ are those calculated by the method C-2-T except where specifically noted otherwise.

STRESS AND STRAIN RELATIONS

The typical relationships between stress ratio σ_1'/σ_3', σ_2'/σ_3' (only in Fig. 6(a)), axial strain ε_a and volumetric strain ε_v for different values of δ at $\sigma_c'=0.05$ kgf/cm^2 and 4.0 kgf/cm^2 are shown in Figs. 6(a) and (b) and in Figs. 7(a) and (b). It may be seen that anisotropy is significant in the strength and deformation characteristics for both dense and loose samples at $\sigma_c'=\sigma_3'=4.0$ kgf/cm^2 (392 kN/m^2) as well as at $\sigma_c'(\fallingdotseq\sigma_3')=0.05$ kgf/cm^2 (4.9 kN/m^2). The results suggest that the deformation during the isotropic compression up to $\sigma_3'=4.0$ kgf/cm^2 (392 kN/m^2) had not altered considerably the fabric of sand with respect to the anisotropic strength and deformation characteristics. It is also noteworthy that even loose samples

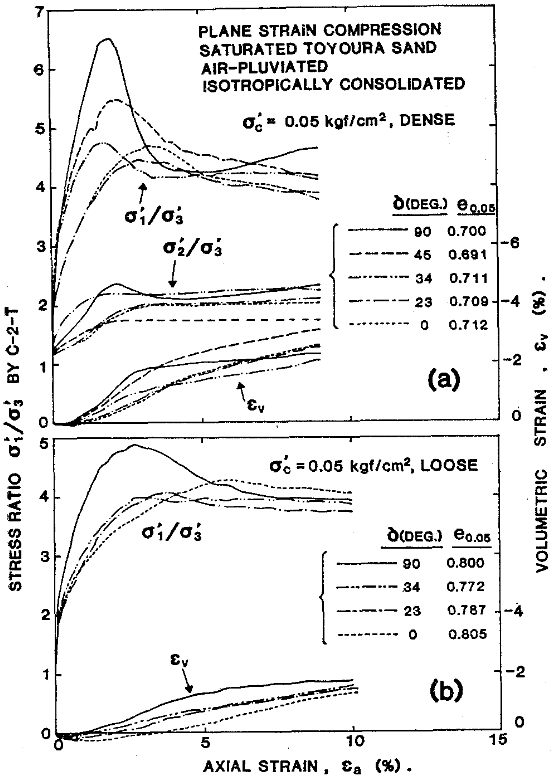

Fig. 6. Typical stress-strain relations for tests at $\sigma_c'=0.05\text{kgf/cm}^2$ for (a) dense and (b) loose samples (Series A)

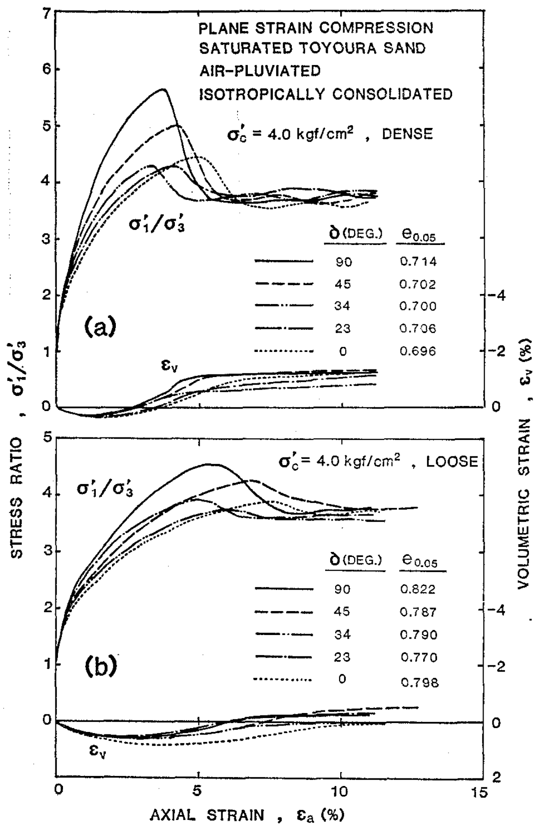

Fig. 7. Typical stress-strain relations for tests at $\sigma_c'=4.0\text{kgf/cm}^2$ for (a) dense and (b) loose samples (Series A)

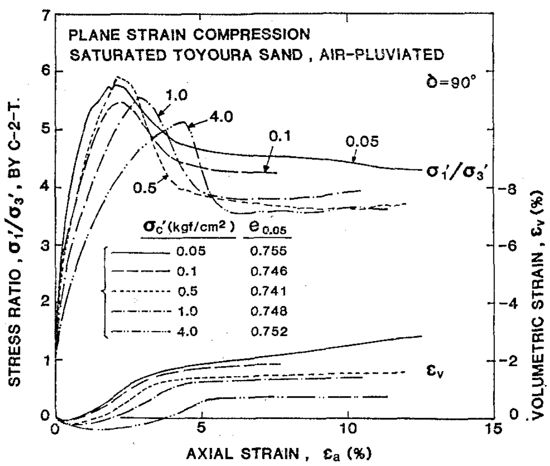

Fig. 8. Comparison of stress-strain relations for different values of σ_c' at $\delta=90°$ for $e_{0.05}\fallingdotseq 0.75$ (Series A)

have a high degree of anisotropy in the strength and deformation characteristics as well as dense samples. It may further be seen that at a larger axial strain where the volume increase is very small, say at $\varepsilon_a=7.5\sim10\%$, the difference in the stress values among different values of δ has almost disappeared.

In Fig. 8 are compared the relationships between σ_1'/σ_3', ε_a and ε_v at different values of σ_c' where $e_{0.05}\fallingdotseq 0.75$ and $\delta=90°$. Concerning the dependency of the deformation characteristics on σ_c', the following three points may be seen from the results. First, the slope $d(\sigma_1'/\sigma_3')/d\varepsilon_a$ at an identical stress ratio level decreases with the increase in σ_c' before the peak stress condition and the axial strain ε_a at the peak stress condition increases with the increase in σ_c', especially at $\sigma_c'\geqq 0.5$ kgf/cm². Secondly, in contrast to this, the rate of the drop of σ_1'/σ_3' or $-d(\sigma_1'/\sigma_3')/d\varepsilon_a$ after the peak stress condition increases with the increase in σ_c'. Lastly, the value of σ_1'/σ_3' at a large axial strain, say $\varepsilon_a= 5\sim10\%$, is larger at a lower σ_c'. Corresponding to this, the rate of volume expansion $-d\varepsilon_v/$

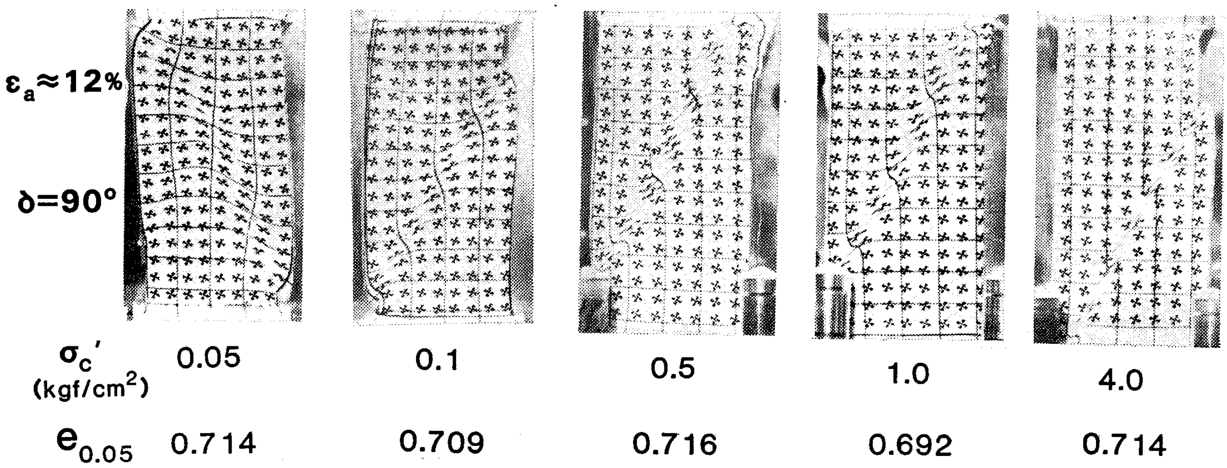

Photo. 1. σ_2'-surfaces at $\varepsilon_a \fallingdotseq 12\%$. Samples are standing under a vacuum with the confining plate of acryl. Targets seen on the membrane are made of latex rubber so that additional resistances to the sample deformation are not produced

$d\varepsilon_a = -1 - d\varepsilon_3/d\varepsilon_1$ at $\varepsilon_a = 5 \sim 10\%$ increases with the decrease in σ_c'. At $\sigma_c' = 0.5$, 1.0 and 4.0 kgf/cm^2, $-d\varepsilon_v/d\varepsilon_a$ at $\varepsilon_a = 5 \sim 10\%$ is almost zero and correspondingly σ_1'/σ_3' is around 3.5 which is close to the slope in the stress-dilatancy relation at $(\sigma_1'/\sigma_3')_{max}$ (Fig. 5) or the value of $(\sigma_1'/\sigma_3')_{max}$ at $-d\varepsilon_3/d\varepsilon_1 = 1.0$ or $-d\varepsilon_v/d\varepsilon_a = 0.0$ in this relation. These indicate that at $\varepsilon_a = 5 \sim 10\%$ some parts in the samples have reached the residual condition when $\sigma_c' = 0.5 \sim 4.0$ kgf/cm^2. On the other hand, at $\sigma_c' = 0.05$ kgf/cm^2 the values of $-d\varepsilon_v/d\varepsilon_a$ is not zero and σ_1'/σ_3' is larger than 3.5 at $\varepsilon_a = 5 \sim 10\%$. This means that at $\sigma_c' = 0.05$ kgf/cm^2 the residual stress condition has not been reached at $\varepsilon_a = 5 \sim 10\%$ even in largely deforming parts within a sample.

In this study, the strain fields on the σ_2'-plane during plane strain compression were measured in detail in the majority of tests (see Photo. 1 for example). It was found that such a dependency of the deformation characteristics on σ_c' as described above is closely related to the dependency on σ_c' of the degree of the uniformity of deformation within samples (Sakamoto et al., 1985 ; Kawamura et al., 1985). Namely, it was observed that a shear band or shear bands start to develop before the peak stress condition and that even before the clear formation of shear bands the deformation within a sample is not uniform with the degree of non-uniformity being larger at a lower σ_c'. In contrast to this, the degree of the concentration of deformation to a shear band or shear bands was larger at a larger σ_c' and the average width of shear band was smaller at a larger σ_c' (see Photo. 1). Therefore, after the peak stress condition for an identical increment of average axial deformation of sample, the shear strain increment in a shear band became larger at a larger σ_c'. Accordingly, it is likely that the residual stress condition is reached by a smaller increment of average axial strain after the peak stress condition at a higher σ_c'. On the other hand it would appear from the observed strain fields that both the relationships between average stresses and average strains based on loads, stresses and displacements measured at boundaries and the uniformity of deformation within a sample, both before and after a shear band or shear bands start to appear, should be considered as a function of both sample dimensions, h/D_{50} (D_{50} is the mean diameter of sand particles) and h/w, and boundary conditions. Such a point as above has been pointed out by Drescher and Vardoulakis (1982) for the case after a shear band or shear bands start to appear. Accordingly, the dependency of the deformation characteristics on σ_c' seen in Fig. 8 should not be considered as a pure material property and should be considered to be strongly affected by the degree of the non-uniformity of deformation within a sample which is a function of σ_c'. The detailed discussions on these points are beyond the scope of this paper.

DEPENDENCY OF φ ON σ_3' AND δ

Dependency of φ on σ_3' : The values of φ obtained by the method C-2-T have been plotted against $e_{0.05}$ for $\delta=90°$ and 23° (Fig. 9). It may be seen that the data points for $\sigma_c'=0.05$, 0.1 and 0.5 kgf/cm² are located within a very narrow band both for $\delta=90°$ and for $\delta=23°$. For $\delta=90°$, average curves of $\varphi\sim e_{0.05}$ relations can be well defined for $\sigma_c'=1.0$ and 4.0 kgf/cm² as denoted by solid curves. The results show that the dependency of φ on σ_3' are very small for a range of $\sigma_3'=0.05\sim0.5$ kgf/cm² both for $\delta=90°$ and 23°. While the data are not presented here, similar trends were seen for the other values of δ examined. In Fig. 10 are compared the values of φ at $\sigma_c'=0.05$ and 0.1 kgf/cm² for $\delta=90°$ calculated by the different methods, U-B and C-2-T or C-4-B and C-2-T. As noted before, the values of φ calculated by the method U-B are the largest possible values of φ and those by the method C-4-B are the smallest possible values of φ. The results shown in Fig. 10 indicate that when the method U-B is employed the dependency of φ on σ_c' becomes slightly larger than it is when the method C-2-T is employed, but this dependency is still not significant. On the other hand, it may be seen that when the method C-4-B is employed, the values of φ at $\sigma_c'=0.05$ kgf/cm² become generally smaller than those at $\sigma_c'=0.1$ kgf/cm². Therefore, it would appear that the method C-4-B is not reasonable, but another method by which larger calculated values of φ are given like the method C-2-T is more reasonable.

Accordingly, in spite of some uncertainties in the calculated values of φ at $\sigma_c'=0.05$ and 0.1 kgf/cm², it can be concluded that

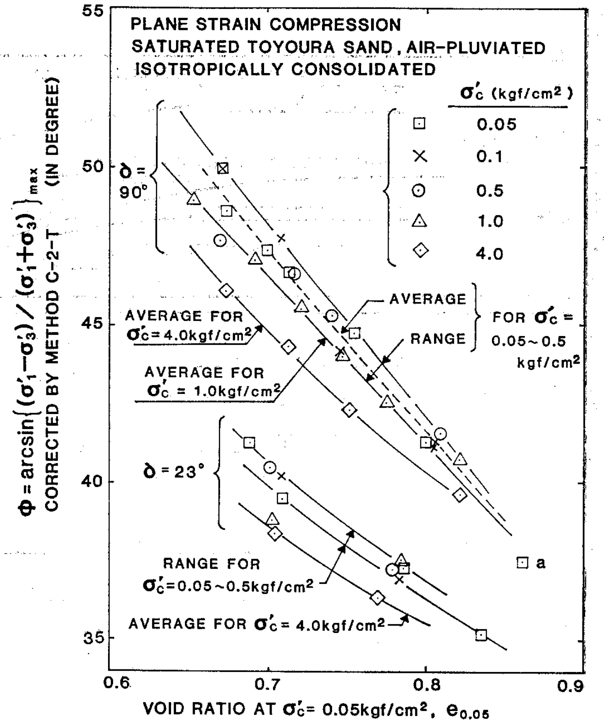

Fig. 9. Relationships between φ by C-2-T and $e_{0.05}$ for $\delta=90°$ and 23° (Series A)

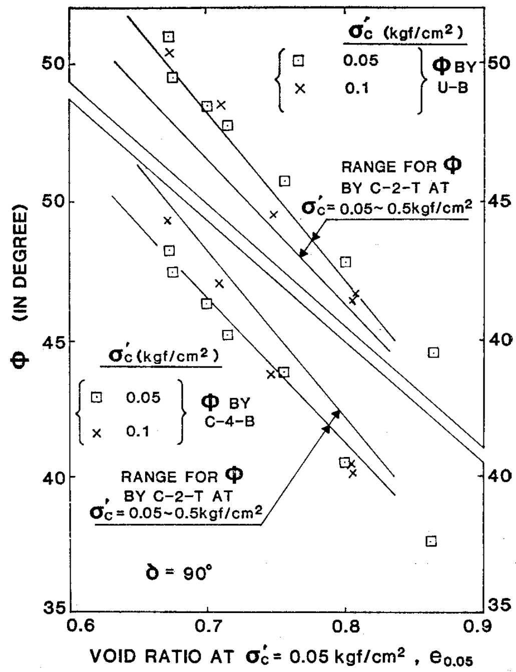

Fig. 10. Comparison of $\varphi\sim e_{0.05}$ relations among different stress calculation methods

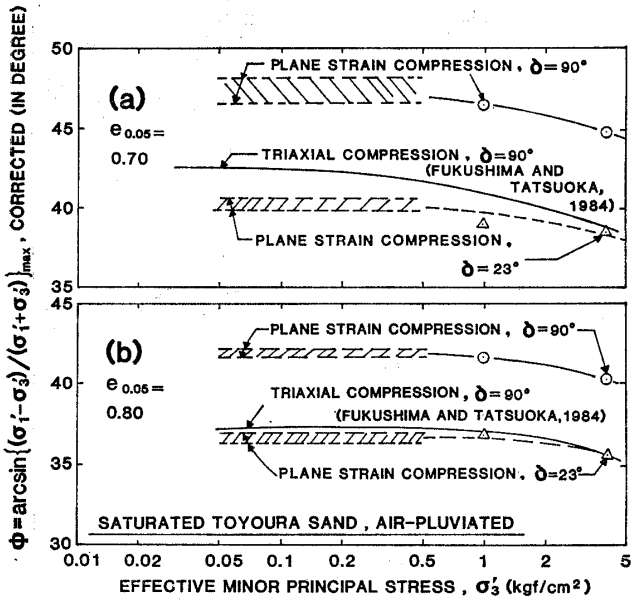

Fig. 11. Relationships between φ and σ_3' (σ_3') at $\delta=90°$ and 23° for $e_{0.05}$=(a) 0.7 and (b) 0.8

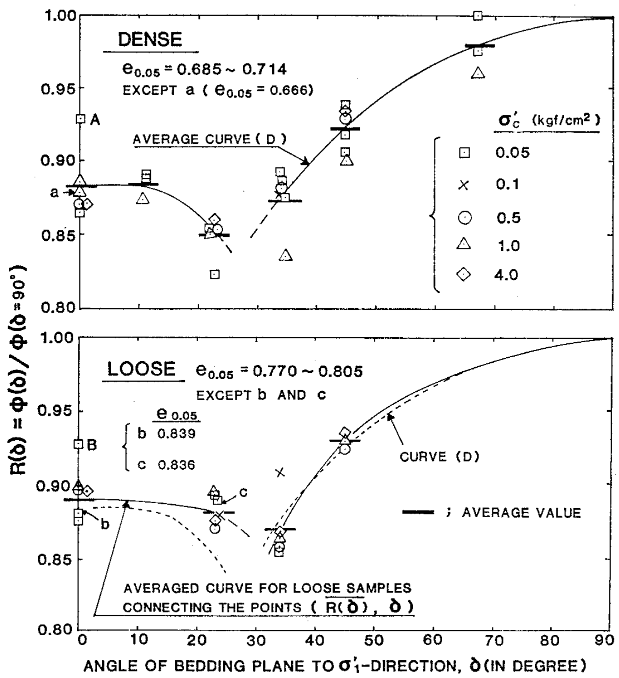

Fig. 12. Relationship between $R(\delta)=\varphi(\delta)/\varphi(\delta=90°)$ and δ (Series A)

the dependency of φ on σ_3' for a range of $\sigma_3'=0.05\sim0.5$ kgf/cm² of saturated Toyoura Sand prepared by the air-pluviation method is negligible, or very small if any, in plane strain compression as well as in triaxial compression.

The range and value of φ at $e_{0.05}=0.7$ and 0.8 were read from the band and the average curves shown in Fig. 9 and plotted against σ_3' in Fig. 11. The relationships for triaxial compression by Fukushima and Tatsuoka (1984) are also shown in Fig. 11. The six relations seen in Fig. 11 show generally similar results in that the dependency of φ on σ_3' is negligible for $\sigma_3'<0.5$ kgf/cm², whereas the value of φ starts to decrease with the increase in σ_3' at around $\sigma_3'=0.5$ kgf/cm².

Dependency of φ on δ (strength anisotropy) : Since a clear dependency of φ on σ_3' cannot be seen for a range of $\sigma_3'=0.05\sim0.5$ kgf/cm², an average relationship between φ and $e_{0.05}$ was defined as well as for σ_3'= 1.0 and 4.0 kgf/cm², which is represented by a broken curve in Fig. 9. Then, the value of φ for each test at δ, $\varphi(\delta)$, other than 90° (0°, 11°, 23°, 34°, 45° and 67°) was divided by φ at $\delta=90°$, $\varphi(\delta=90°)$ or $\varphi(\delta=90°$, PSC) at the same $e_{0.05}$ as the test. $\varphi(\delta=90°)$ are given by either of three averaged curves for $\delta=90°$ in Fig. 9. The ratios $R(\delta)=\varphi(\delta)/\varphi(\delta=90°)$ in plane strain compression at all the values of σ_c' employed in this study have been plotted against δ (Figs. 12(a) and (b)) or against $e_{0.05}$ (Fig. 13). Furthermore, these ratios at $\sigma_3'=1.0$ kgf/cm² in plane strain compression were plotted against δ together with those in triaxial compression in Fig. 14. The values of φ at $\delta=90°$ in triaxial compression for $e_{0.05}$= 0.7 and 0.8 were obtained from Fukushima and Tatsuoka (1984) where cylindrical samples were used and those at $\delta=0°$ were obtained by this study using rectangular prism samples ($h_0\times w_0\times l_0=8.0\times4.3\times8.0$ cm) as used for the plane strain compression tests in Series B. The relation for triaxial compression at $e=0.67\sim0.68$ was obtained from the results by Oda et al. (1978) where $\varphi(\delta=90°$, PSC$)=50.4°$ is reported. Several points may be seen from Figs. 12 through 14.

First, there is strong anisotropy in φ in both loose and dense samples and φ has a minimum somewhere between $\delta=23°$ and 34°. Furthermore, it may be seen in Fig. 12 that the scattering in the data points except

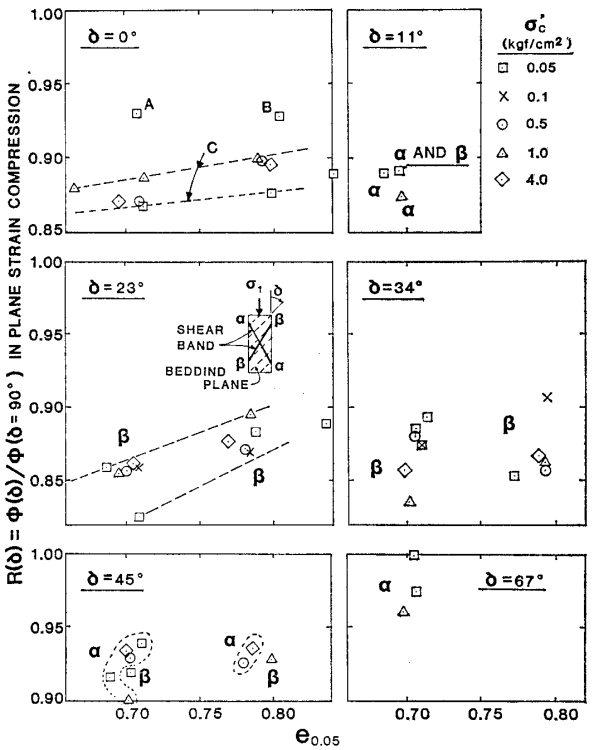

Fig. 13. Relationships between $R(\delta)=\varphi(\delta)/\varphi(\delta=90°)$ and $e_{0.05}$ at different values of δ (Series A)

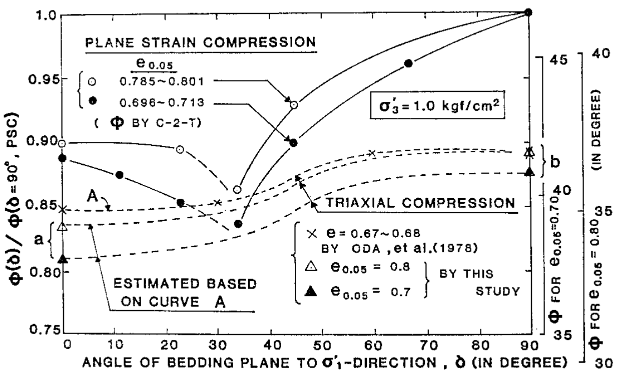

Fig. 14. Relationship between $R(\delta)=\varphi(\delta)/\varphi(\delta=90°$, PSC) and δ at $\sigma_3'=1.0\,\mathrm{kgf/cm^2}$

two points at $\delta=0°$ and $\sigma_c'=0.05\,\mathrm{kgf/cm^2}$ which are labelled A and B is not materially large and the dependency of the ratio $R(\delta)$ on σ_c' is not discernible. It seems to be a very important finding that such anisotropic characteristics of strength as seen in Figs. 12 through 14 are preserved even at such a relatively high pressure as $\sigma_3'=4.0\,\mathrm{kgf/cm^2}$ ($392\,\mathrm{kN/m^2}$) as well as at such a very low pressure as $\sigma_3'=0.05\,\mathrm{kgf/cm^2}$ ($4.9\,\mathrm{kN/m^2}$).

A solid curve seen in Fig. 12(a) and Fig. 12(b) represents an average relationship between $R(\delta)$ and δ for a range of $\sigma_3'=0.05\sim4.0\,\mathrm{kgf/cm^2}$.

Next, it may be seen that the degree of strength anisotropy in terms of $R(\delta)=\varphi(\delta)/\varphi(\delta=90°)$ is only slightly less in looser sand than in denser sand. Therefore, it seems that even in model tests under the plane strain condition using air-pluviated loose sand the strength anisotropy plays an important role as well as in those with air-pluviated dense sand.

Furthermore, the results shown in Fig. 14 seem to suggest that at δ between 23° and 34° φ in plane strain compression is similar to that in triaxial compression. This result means that the dependency of φ on the parameter $b=(\sigma_2'-\sigma_3')/(\sigma_1'-\sigma_3')$ is a strong function of δ, with this dependency being the largest at $\delta=90°$ and the smallest or even none at δ where φ in plane strain compression has its minimum. Further studies at wider ranges of b and σ_c' will be needed to clarify this point.

It was suggested by Arthur and Dunstan (1978), Matsuoka et al. (1984) and Haruyama and Kitamura (1984) that the strength anisotropy is a function of the smaller one of two angles between the stress characteristics at failure and the bedding plane, $\delta-\varepsilon(\delta)$ (see the inset in Fig. 15) where the angle $\varepsilon(\delta)$ is equal to $45°-\varphi(\delta)/2$. The absolute value (>0) of the angle $\delta-\varepsilon(\delta)$ at each δ was divided by its value at $\delta=90°$, $\{90°-\varepsilon(\delta=90°)\}=45°+\varphi(\delta=90°)/2$. Then all the data were summarized in a normalized relationship between $R(\delta)=\varphi(\delta)/\varphi(\delta=90°)$ and $x=|\delta-\varepsilon(\delta)|/\{90°-\varepsilon(\delta=90°)\}$ (Fig. 15). Note that for $\delta=45°$ and 0° the parameter x becomes a similar value. It may be seen that all the data points are located within a band except for those designated by the letter C which are the majority of data points at $\delta=0°$ for $\sigma_c'=0.5\sim4.0\,\mathrm{kgf/cm^2}$. For this band the ratio $R(\delta)$ increases monotonously with the increase in the parameter x. It may also be seen that for $\delta=0°$ only two data points for $\sigma_c'=0.05\,\mathrm{kgf/cm^2}$ labelled

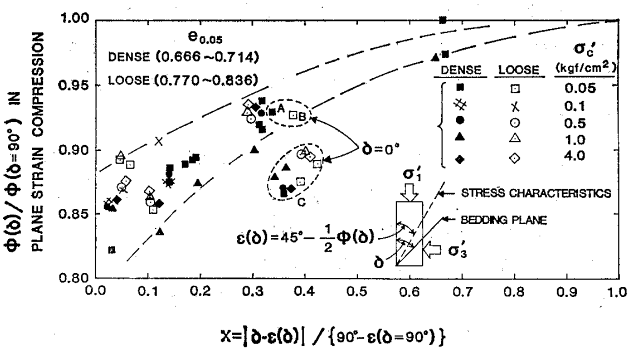

Fig. 15. Relationship between $R(\delta)=\varphi(\delta)/\varphi(\delta=90°)$ and parameter x

A and B are located within this band. Furthermore, it may be seen that the scattering in the data is not less than that seen in Fig. 12. Accordingly, it would appear from these results that the strength anisotropy in terms of $R(\delta)=\varphi(\delta)/\varphi(\delta=90°)$ is not necessarily a unique function of the parameter x.

Another inconsistency was observed with respect to relating the degree of strength anisotropy directly to the parameter x as follows. At δ other than 0° and 90°, two kinds of shear bands are kinematically possible ; the one having a larger angle to the bedding plane and the other having a smaller angle to the bedding plane which are designated by $\alpha-\alpha$ and $\beta-\beta$ in the inset of Fig. 13. In Fig. 13, the letters α or β indicate the types of shear band, $\alpha-\alpha$ or $\beta-\beta$. When it is assumed that the strength anisotropy is uniquely controlled by the parameter x, it would appear reasonable to anticipate that only shear bands of the type $\beta-\beta$ appear. At $\delta=23°$ and 34°, all the shear bands observed were of the type $\beta-\beta$. However, at $\delta=45°$, both types of shear bands appeared and any clear difference in φ between two types of shear bands was not observed. At $\delta=11°$ and 67°, the majority of shear bands were of the type $\alpha-\alpha$. Therefore, it would appear that the strength anisotropy observed in plane strain compression cannot be directly related to the direction of shear band with respect to the bedding plane as represented by the parameter x.

The average relations shown in Figs. 12(a) and (b) may be very useful to evaluate the value of φ at δ other than 90° from the value of φ at $\delta=90°$ which is most easily obtained by the conventional plane strain compression tests.

EFFECTS OF INITIAL STRESS CONDITION ON φ

To evaluate the extent of the effects of the initial stress ratio $(\sigma_1'/\sigma_3')_c$ at the start of plane strain compression, the relationships between σ_1'/σ_3', ε_a and ε_v were directly compared at an identical value of $\sigma_3'(=0.5$ kgf/cm²) between isotropically and anisotropically consolidated samples $(K=(\sigma_3'/\sigma_1')_c=1.0$ and $K=K_0$, Fig. 16). For direct comparisons, the origin of the curve for an anisotropically consolidated sample designated by the letter S was located on the point on the curve for an isotropically con-

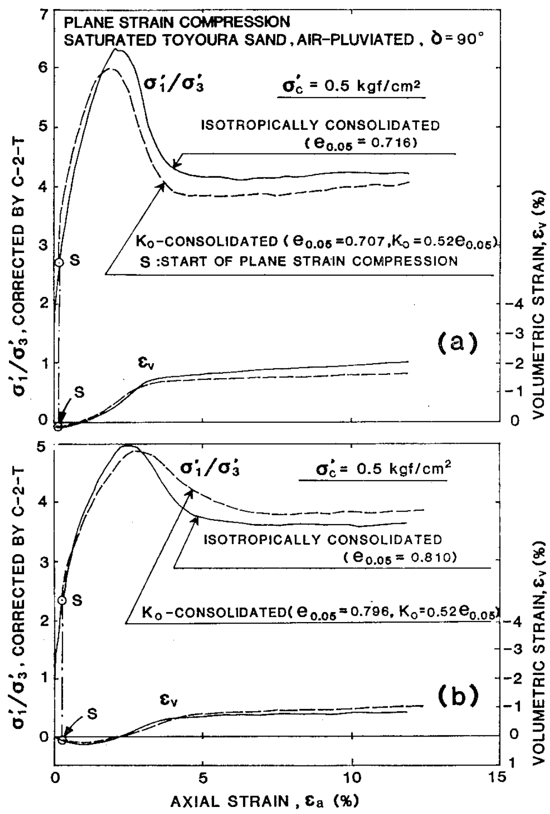

Fig. 16. Comparisons of stress-strain relations between isotropically and anisotropically consolidated samples at $\delta=90°$ and $\sigma_c'=0.5$kgf/cm² (Series A)

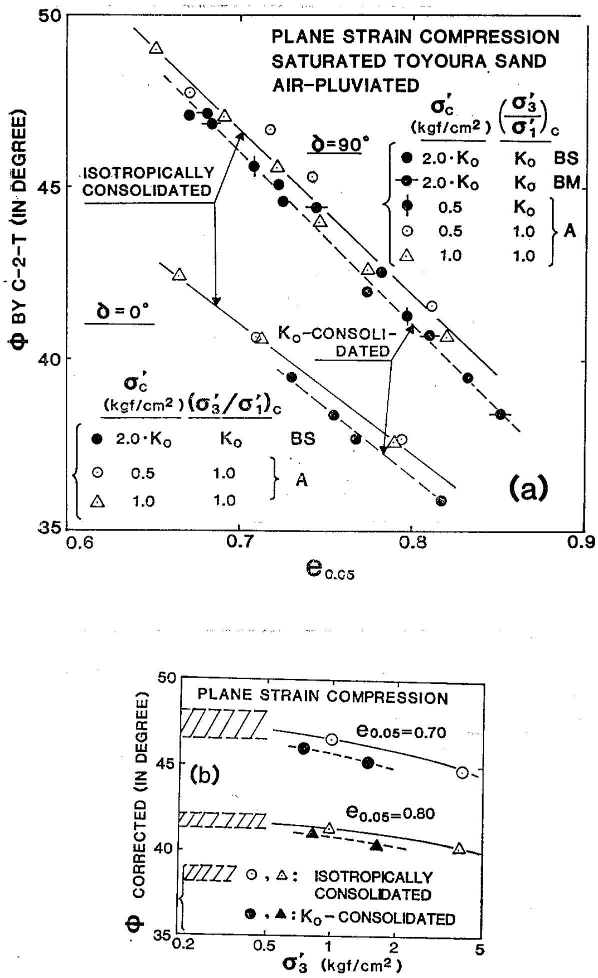

Fig. 17. (a), (b) **Effects of initial stress ratio on φ for $\delta=90°$ and $\delta=0°$**

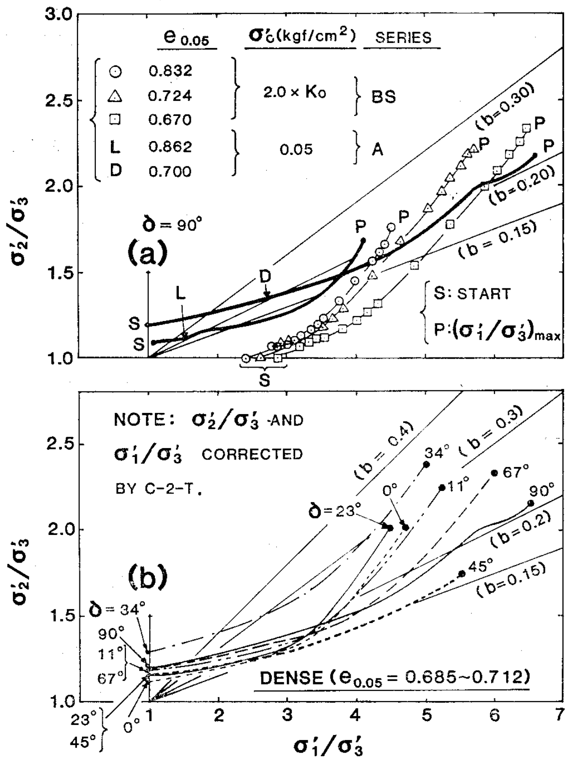

Fig. 18. Stress paths in terms of σ_2'/σ_3' and σ_1'/σ_3' ; (a) effects of initial stress condition and (b) effects of δ (Series A and B)

solidated sample where $\sigma_1'/\sigma_3'=1/K_0$. It may be seen that the general shape of the relation is quite similar between two kinds of samples. The values of φ at $\delta=90°$ and $0°$ for anisotropically and isotropically consolidated samples are summarized in Fig. 17(a) and (b). The values of σ_3' for anisotropically consolidated samples are between 0.5 and 1.0 kgf/cm² and those for isotropically consolidated samples are 0.5 or 1.0 kgf/cm². It may be seen that the effects of initial stress ratio on φ can be discernible while the difference is not larger than 1 degree. The difference in φ may be due to possible differences in the value of σ_2'/σ_3' at the peak stress condition which result from the differences in σ_2'/σ_3' when $\sigma_1'/\sigma_3'=1/K_0$ (at the point S in Fig. 16). It is unfortunate that the values of σ_2' were not measured for the results shown in Fig. 16. In Fig. 18 (a) are compared the stress paths in terms of σ_2'/σ_3' and σ_1'/σ_3' between anisotropically and isotropically consolidated samples, while the value of σ_3' is not the same between them, $2.0\times K_0 \fallingdotseq 0.7\sim 0.8$ kgf/cm² or 0.05 kgf/cm². The reason why the values of σ_2'/σ_3' at the start of test designated by the letter S for isotropically consolidated samples are larger than 1.0 is that some amount of seating stress was introduced at the setting of the confining plates (CFP, Fig. 2(a)). The results seem to be suggesting that the initial stress difference between two kinds of samples is going to disappear with straining. However, in the case where initial stress difference still remains to some extent at the peak stress condition, the ratio σ_2'/σ_3' can be larger for an isotropically consolidated sample than for an anisotropically consolidated sample, resulting in a slightly larger φ for an isotropically consolidated sample than for an anisotropically consolidated one. However, any clear conclusion concerning the effects of the initial stress ratio on the value of b at failure cannot be obtained from Fig. 18 (a) since the values of σ_3' were very different for different initial stress ratios in these data. Further research will be needed to clarify how the initial stress condition influences the value of φ.

THE INTERMEDIATE PRINCIPAL STRESS

The relative magnitude of σ_2' to σ_1' and σ_3' is conventionally represented either by the parameter $b=(\sigma_2'-\sigma_3')/(\sigma_1'-\sigma_3')$ which is the slope of a straight line originated from the point (1, 1) in the stress plane in Fig. 18 or the ratio $a=\sigma_2'/s$ in which $s=(\sigma_1'+\sigma_3')/2$ (Cornforth, 1964). The values a and b at $(\sigma_1'/\sigma_3')_{max}$ in the tests at $\delta=90°$ have been plotted against $e_{0.05}$ (Fig. 19(a)). Cornforth (1964) reported that the parameter a varied from approximately 0.54 for the denser specimens to 0.72 for the looser specimens. A similar trend may be seen in the data shown in Fig. 19(a).

On the other hand, it may be seen in Fig. 18(b) that the shape of stress path is strongly affected by δ. In particular, the variation when δ changes from 45° to 34° is quite large. Consequently, the relationships at the peak stress condition between b and δ and between a and δ have also a sort of discontinuity between $\delta=34°$ and 45° (Fig. 19(b)). Such characteristics should be explained by the anisotropic deformability of specimens.

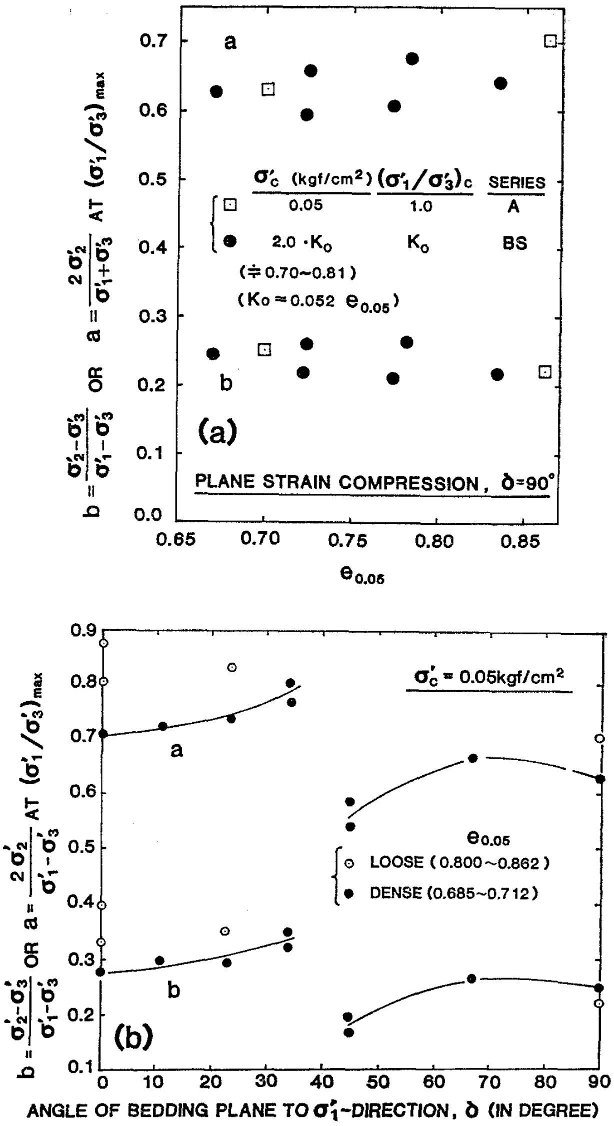

Fig. 19. Parameters $b=(\sigma_2'-\sigma_3')/(\sigma_1'-\sigma_3')$ and $a=2\sigma_2'/(\sigma_1'+\sigma_3')$ at $(\sigma_1'/\sigma_3')_{max}$ plotted against (a) $e_{0.05}$ for tests at $\delta=90°$ and (b) δ for tests at $\sigma_c'=0.05$kgf/cm² (Series A and B)

STRESS-DILATANCY RELATION AT PEAK

The data points of stress dilatancy relations in terms of σ_1'/σ_3' and $-d\varepsilon_3/d\varepsilon_1$ at the peak stress condition in the plane strain compression tests (PSC) of Series A are shown in Fig. 5 and Figs. 20(a) through (e). Three data points (two at $\delta=90°$ and one at $\delta=45°$) for $\sigma_c'=1.0$ kgf/cm² have been omitted since very accurate volume change measurements were failed in these tests. However, it was confirmed that this kind of inaccuracy did not influence the calculated values of φ which have been used in this paper. The range of the data for $\delta=90°$ shown in Fig. 5 is represented by a band in each of Figs. 20(a) through (e). The range for the triaxial compression tests (TC) at $\delta=90°$ obtained by Fukushima and Tatsuoka (1984) is also indicated by a band in Fig. 20. The data points for the triaxial compression tests at

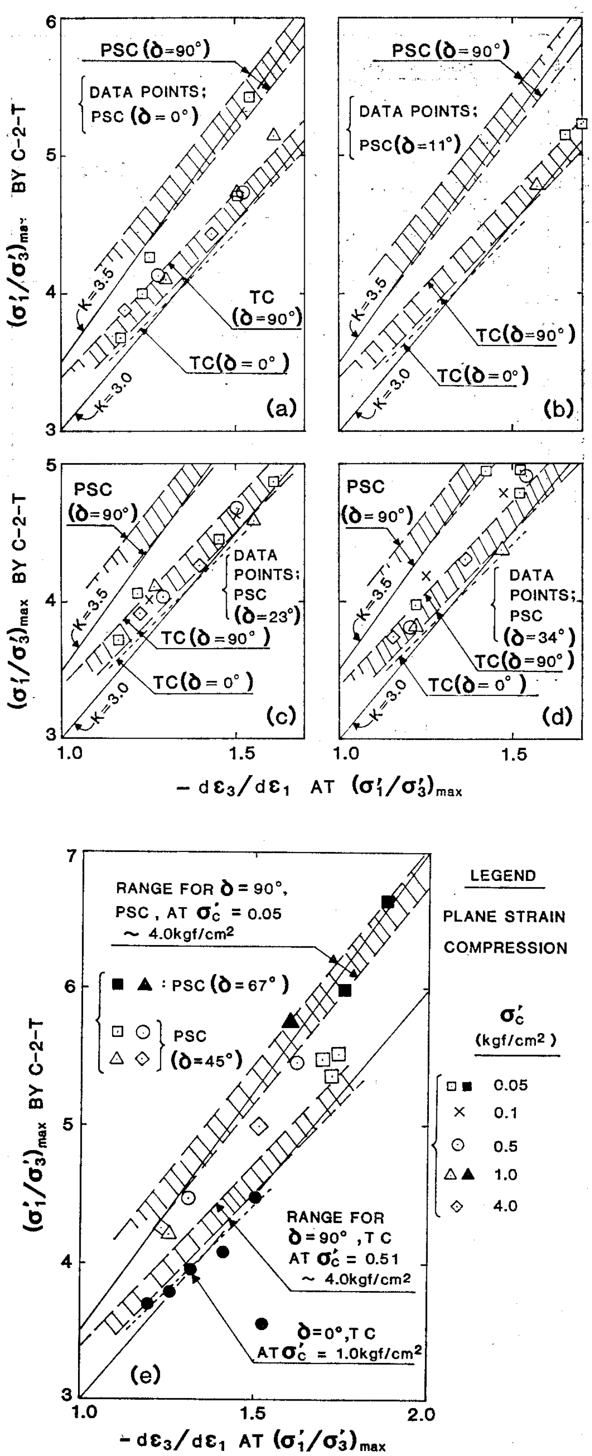

Fig. 20. Stress-dilatancy relations at peak in plane strain compression for (a) $\delta=0°$, (b) $\delta=11°$, (c) $\delta=23°$, (d) $\delta=34°$ and (e) $\delta=45°$ and $67°$ (Series A)

$\delta=0°$ obtained by this study are also shown in Fig. 20(e) and its average relation denoted by a broken line is also shown in each

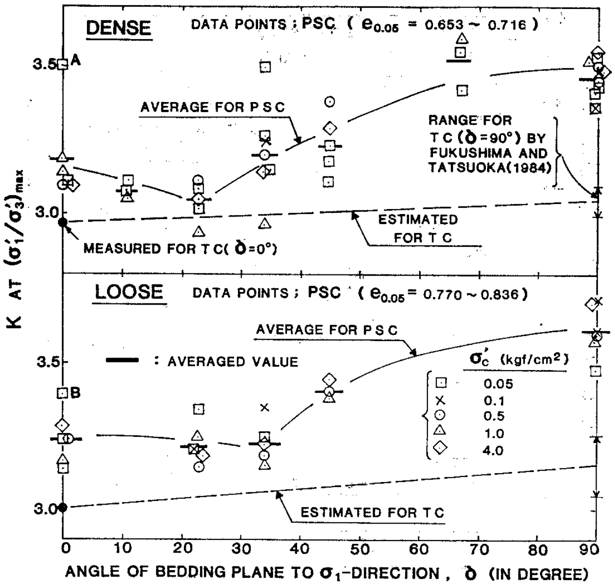

Fig. 21. Ratio $K=(\sigma_1'/\sigma_3')/(-d\varepsilon_3/d\varepsilon_1)$ at peak as a function of δ

of Figs. 20(a) through (d). The results show clearly that while the stress-dilatancy relation at failure in plane strain compression is rather independent of σ_c' at each δ, this relationship is strongly influenced by δ. In contrast, it seems that in triaxial compression the stress-dilatancy relationships at the peak stress condition are rather insensitive to δ as has been shown by Oda (1972).

The ratios $K=(\sigma_1'/\sigma_3')/(-d\varepsilon_3/d\varepsilon_1)$ at the peak stress condition for dense and loose samples are shown as a function of δ in Fig. 21. While scattering of the data for plane strain compression is not small, averaged values of K were calculated at each δ and average relations were defined as represented by solid curves. For the case of triaxial compression, straight lines were connected only expediently between the data points at $\delta=0°$ and those at $\delta=90°$ since the data except for $\delta=0°$ and $90°$ were not available. The results show that the parameter K in plane strain compression is a strong function of δ as well as φ. At the same time, it may be seen that the difference in K between plane strain compression and triaxial compression is very small at the value of δ where φ has its minimum in plane strain compression.

In model tests under the plane strain condi-

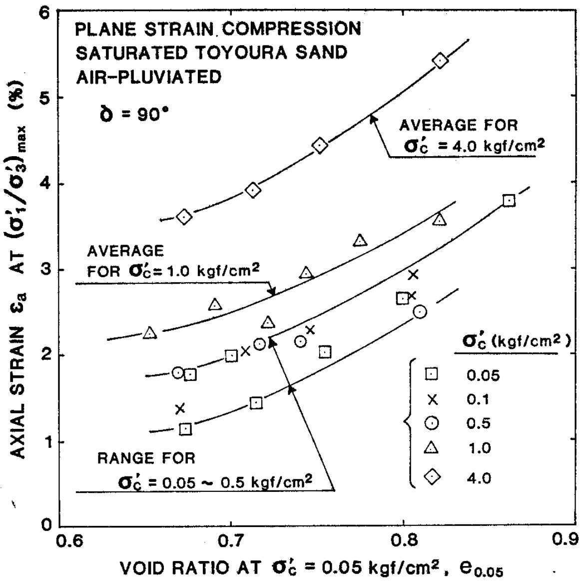

Fig. 22. Axial strain at $(\sigma_1'/\sigma_3')_{max}$ at $\delta=90°$ as a function of $e_{0.05}$ (Series A)

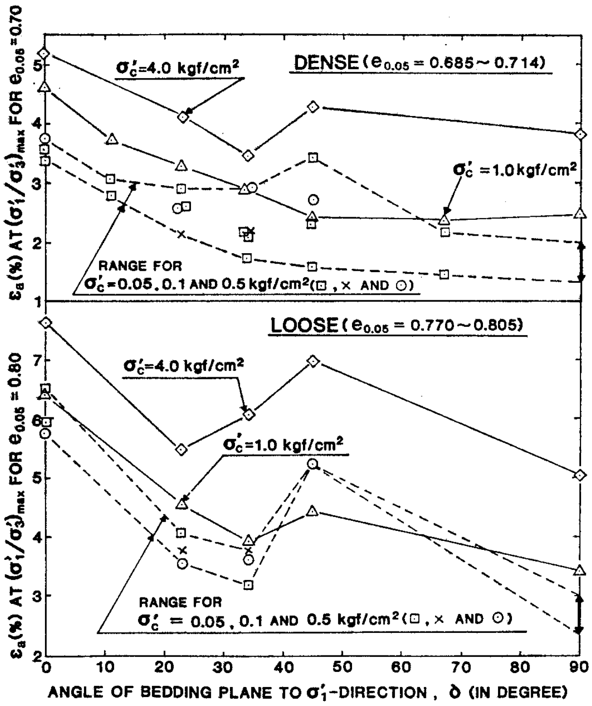

Fig. 23. Axial strain at $(\sigma_1'/\sigma_3')_{max}$ as a function of δ (Series A)

tion such as bearing capacity tests of strip footing on sand, only the distribution of $-d\varepsilon_3/d\varepsilon_1$ on the σ_2'-plane within a sand mass can be measured. The curves shown in Fig. 21 may be useful to estimate the local values of σ_1'/σ_3' from measured values of $-d\varepsilon_3/d\varepsilon_1$ through the stress-dilatancy relation ; $\sigma_1'/\sigma_3'=K\cdot(-d\varepsilon_3/d\varepsilon_1)$ with accounting for the effects of stress path on this relation. It has been shown by Tatsuoka (1980) that the effect of stress path on the stress-dilatancy relation becomes smaller or even negligible at larger strains or near and at the failure condition.

DEFORMATION CHARACTERISTICS

The average axial strain by boundary displacements at $(\sigma_1'/\sigma_3')_{max}$ for $\delta=90°$ are shown in Fig. 22. It may be seen that at one density the axial strain at $(\sigma_1'/\sigma_3')_{max}$ starts increasing considerably with the increase in σ_c' at around $\sigma_c'=0.5$ kgf/cm². This tendency is similar to that seen for φ (Fig. 9). Furthermore, this tendency has also been observed in triaxial compression (Fukushima and Tatsuoka, 1984). Accordingly, it would appear from these results that the deformation characteristics before the peak stress condition does not change significantly by the change in σ_3' for $\sigma_3'<0.5$ kgf/cm² as well as the value of φ.

Axial strains at $(\sigma_1'/\sigma_3')_{max}$ for $e_{0.05}=0.70$ or 0.80 are shown as a function of δ in Fig. 23. When $e_{0.05}$ for a test was not exactly equal to 0.70 or 0.80, the measured value of axial strain was corrected for the difference of $e_{0.05}$ from 0.70 or 0.80 using the relations shown in Fig. 22. However, the amount of correction was 8% at largest. At $\delta=90°$ for $\sigma_c'=0.05\sim0.5$ kgf/cm² only the ranges are indicated based on the results shown in Fig. 22. Fig. 24 shows average axial strains by boundary displacements observed at $\sigma_1'/\sigma_3'=3.0$ at various values of δ where average curves have been defined only for $\delta=0°$ and 90°. The results show clearly that at any value of σ_c' between 0.05 and 4.0 kgf/cm² the deformability of sample in terms of the axial strains at $(\sigma_1'/\sigma_3')_{max}$ or at $\sigma_1'/\sigma_3'=3.0$ is not the largest at δ between 23° and 34° where φ has its minimum, but the deformability is the largest at $\delta=0°$. This trend can be noticed also in Figs. 6 and 7. In particular, it may be seen in Fig. 6(a) that at $\delta=34°$ the sample

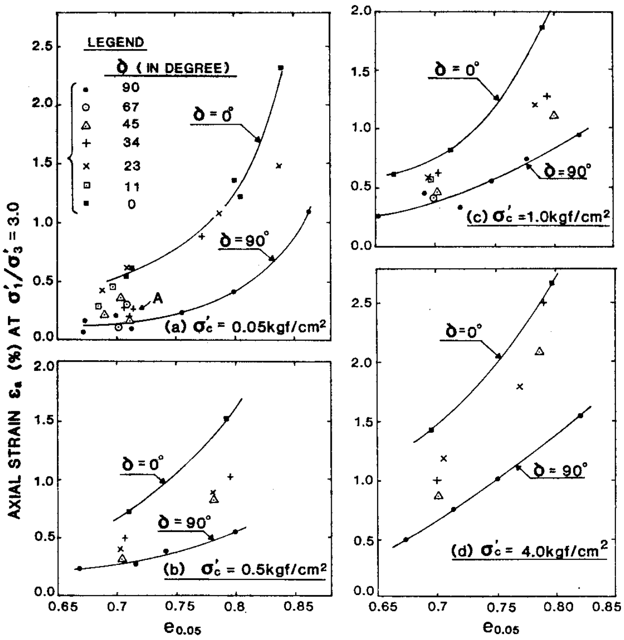

Fig. 24. Axial strain at $\sigma_1'/\sigma_3'=3.0$ (Series A)

has a small deformability and a small strength. Accordingly, it is apparent that the deformability of sample with the dimensions and boundary conditions employed in this study does not increase monotonously with the decrease in the parameter x (Fig. 15). It was found that several points described above concerning the deformation characteristics are also valid when the deformability of sample is expressed in terms of $\gamma_{max}=\varepsilon_1-\varepsilon_3$ and $\varepsilon_v=\varepsilon_1+\varepsilon_3$. Further studies will be needed to clarify whether or not the dependency of deformability on δ seen in Figs. 23 and 24 is influenced by the sample dimensions and/or boundary conditions.

CONCLUSIONS

On the basis of the limited number of plane strain compression tests on saturated Toyoura Sand reported in this paper, the following was found :

(1) In spite of some uncertainties in the determination of stress values in the tests at $\sigma_c'=0.05$ and $0.1\ \mathrm{kgf/cm^2}$, it can be concluded that the dependency of φ on σ_3' for a stress range of $\sigma_3'=0.05\sim0.5\ \mathrm{kgf/cm^2}$ is very small in plane strain compression as well as in triaxial compression.

(2) The strength anisotropy in plane strain compression defined as the ratio of φ at δ (the angle of bedding plane to the σ_1'-direction) to φ at $\delta=90°$ is rather insensitive to the changes both in sample density and in the confining pressure σ_3' between 0.05 and $4.0\ \mathrm{kgf/cm^2}$. The minimum values of φ were recorded for $\delta=23°\sim34°$ and this minimum value of φ seems very similar to the value of φ at that δ in triaxial compression.

(3) The stress-dilatancy relation $\sigma_1'/\sigma_3'=K(-d\varepsilon_3/d\varepsilon_1)$ at the peak stress condition in plane strain compression is strongly influenced by δ whereas this is not in triaxial compression. At $\delta=90°$, the parameter K at the peak stress condition is approximately 3.5 in plane strain compression as compared with approximately $3.0\sim3.1$ in triaxial compression. However, the parameter K in plane strain compression has its minimum value for $\delta=23°\sim34°$ and this value becomes similar to that in triaxial compression.

(4) The deformability of sample in terms of the axial strain value at $\sigma_1'/\sigma_3'=3.0$ or $(\sigma_1'/\sigma_3')_{max}$ does not change so much with the change in σ_3' for $\sigma_3'=0.05\sim0.5\ \mathrm{kgf/cm^2}$, while this starts increasing considerably with the increase in σ_3' at approximately $\sigma_3'=0.5\ \mathrm{kgf/cm^2}$. This tendency corresponds well to the dependency of φ on σ_3'.

(5) For the sample dimensions and the boundary conditions employed in this study, the axial strain at $(\sigma_1'/\sigma_3')_{max}$ or one value of σ_1'/σ_3' before the peak stress condition is not the largest for $\delta=23°\sim34°$ but is the largest at $\delta=0°$. Accordingly, the strength anisotropy and the deformation anisotropy are somewhat different.

ACKNOWLEDGEMENTS

The authors gratefully acknowledge the helpful cooperation provided by Messrs. Y. Futaba and T. Sato and Miss M. Torimitsu. The authors are indebted to Prof. M. Oda of the Saitama University who provided them helpful suggestions. The authors would also like to acknowledge Dr. F. Molenkamp, the Delft Soil Mechanics Laboratory the Netherlands, for reviewing the manuscript. Financial support provided by the Ministry of Education is also greatly acknowledged.

REFERENCES

1) Arthur, J. R. F. and Assadi, A. (1977) : "Ruptured sand sheared in plane strain," Proc. 9 th ICSMFE, Tokyo, Vol. 1, pp. 19-22.
2) Arthur, J. R. F. and Dunstan, T. (1978) : Discussion, Soils and Foundations, Vol. 18, No. 4, pp. 105-106.
3) Becker, E., Chan, C. K. and Seed, H. B. (1972) : "Strength and deformation characteristics of rockfill materials in plane strain and triaxial compression tests," Report No. TE-72-3, Dept. of Civil Eng., Univ. of California, Berkeley.
4) Cornforth, D. H. (1964) : "Some experiments on the influence of strain conditions on the strength of sand," Géotechnique, Vol. 14, No. 2, pp. 143-167.
5) Drescher, A. and Vardoulakis, I. (1982) : "Geometric softening in triaxial tests on granular material," Géotechnique, Vol. 32, No. 4, pp. 291-303.
6) Duncan, J. M. and Seed, H. B. (1967) : "Corrections for strength test data," Jour. of SMF Div., Proc. ASCE, Vol. 93, No. SM 5, Sept., pp. 121-137.
7) Fukushima, S. and Tatsuoka, F. (1984) : "Strength and deformation characteristics of saturated sand at extremely low pressures," Soils and Foundations, Vol. 24, No. 4, pp. 30-48.
8) Haruyama, M. and Kitamura, R. (1984) : "Anisotropic deformation-strength properties of soft sedimentary rock "Shirasu" originated from pyroclastic flows," Soils and Foundations, Vol. 24, No. 4, pp. 84-94.
9) Kawamura, T., Tatsuoka, F. and Sakamoto, M. (1985) : "On stress-strain relations from local strain distributions in plane strain compression on sand," Proc. Annual Symp., Japanese Society of Civil Engineers, Sendai, III-218, pp. 435-436 (in Japanese).
10) Kimura, T., Kusakabe, O. and Saitoh, K. (1984) : "Geotechnical model tests of bearing capacity problems in a centrifuge," Géotechnique, Vol. 35, No. 1, pp. 33-45.
11) Matsuoka, H., Hirao, J. and Fukutake, Y. (1984) : "Deformation and failure of anisotropic sand deposits," Tsuchi-to-Kiso, JSSMFE, Ser. No. 322, Vol. 32, No. 11 (in Japanese).
12) Oda, M. (1972) : "The mechanism of fabric changes during compressional deformation of sand," Soils and Foundations, Vol. 12, No. 2, pp. 1-18.
13) Oda, M., Koishikawa, I. and Higuchi, T. (1978) : "Experimental study on anisotropic shear strength of sand by plane strain test," Soils and Foundations, Vol. 18, No. 1, pp. 25-38.
14) Oda, M. (1981) : "Anisotropic strength of cohesionless sands," Jour. GE Div., Proc. ASCE, Vol. 107, No. GT 9, Sept., pp. 1219-1231.
15) Okochi, Y. and Tatsuoka, F. (1984) : "Some factors affecting K_0-values of sand in triaxial cell," Soils and Foundations, Vol. 24, No. 3, pp. 52-68.
16) Rowe, P. W. (1962) : "The stress-dilatancy relations for static equilibrium of an assembly of particles in contact," Proc. of the Royal Society, Vol. 269, Series A, London, pp. 500-527.
17) Sakamoto, M., Tatsuoka, F. and Kawamura, T. (1985) : "On shear bands in plane strain compression tests on sands," Proc. Annual Symp., Japanese Society of Civil Engineers, Sendai, III-217, pp. 433-434 (in Japanese).
18) Tani, Y., Hatamura, Y. and Nagao, T. (1983) : "Development of small three-component dynamometer for cutting force measurement," Bulletin of the Japanese Society of Mechanical Eng., Vol. 26, No. 214, April, pp. 650-658.
19) Tatsuoka, F. (1980) : "Stress-strain behavior of an idealized anisotropic granular material," Soils and Foundations, Vol. 20, No. 3, pp. 75-90.
20) Tatsuoka, F., Molenkamp, F., Torii, T. and Hino, T. (1984) : "Behavior of lubrication layers of platens in element tests," Soils and Foundations, Vol. 24, No. 1, pp. 113-128.
21) Tatsuoka, F., Goto, S. and Sakamoto, M. (1986) : "Effects of some factors on strength and deformation characteristics of sand at low pressures," Soils and Foundations, Vol. 26, No. 1, pp. 105-114.
22) van Leussen, W. and Nieuwenhuis, J. D. (1984) : "Soil mechanics aspects of dredging," Géotechnique, Vol. 34, No. 3, pp. 359-381.
23) Yamaguchi, H., Kimura, T. and Fuji-i, N. (1979) : Closure, Soils and Foundations, Vol. 19, No. 1, pp. 93-95.